

Assessment Figures and Tables

by

Rachel Mugumo

(15295827)

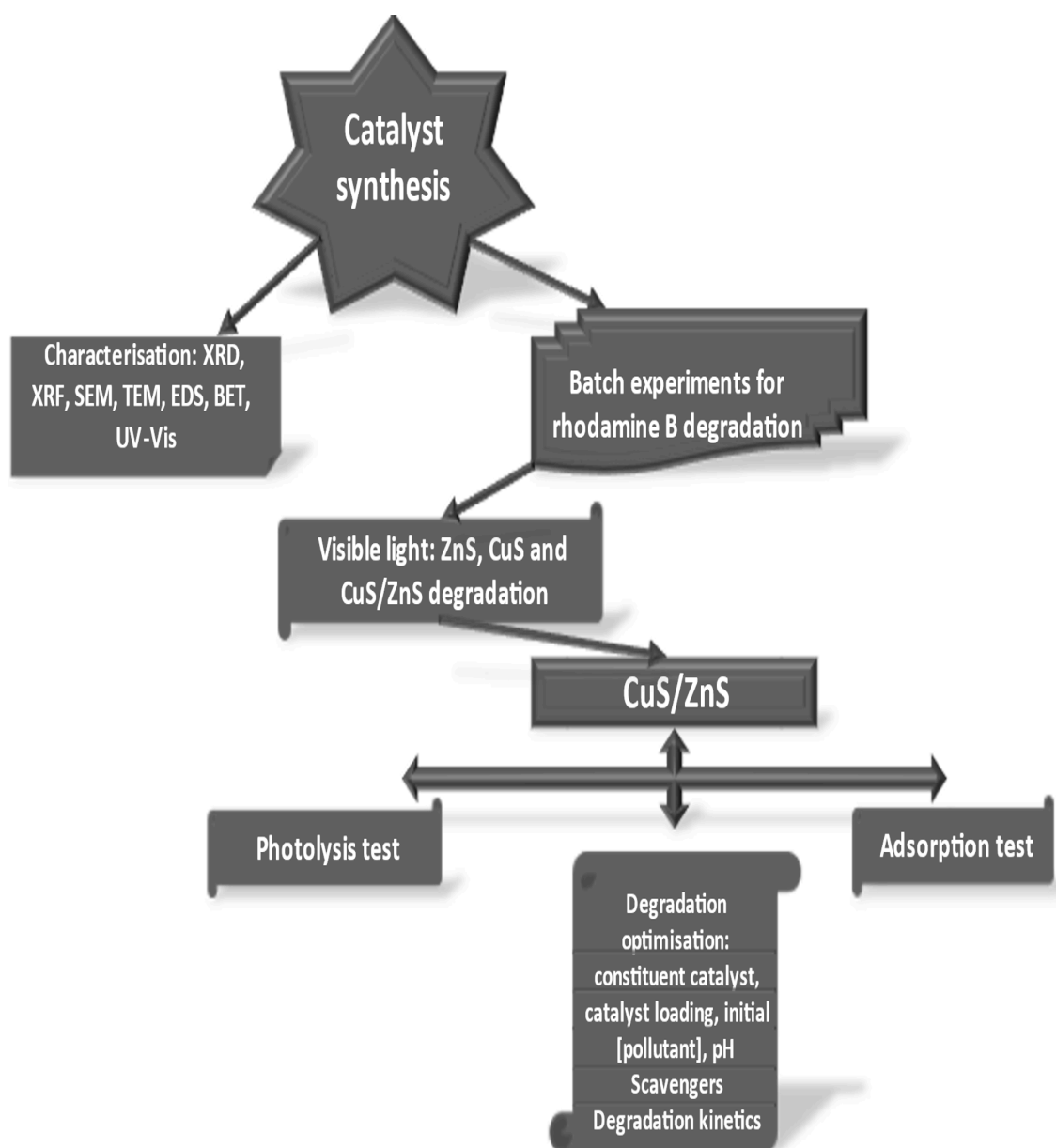


Figure 1.1: Research study plan outline.

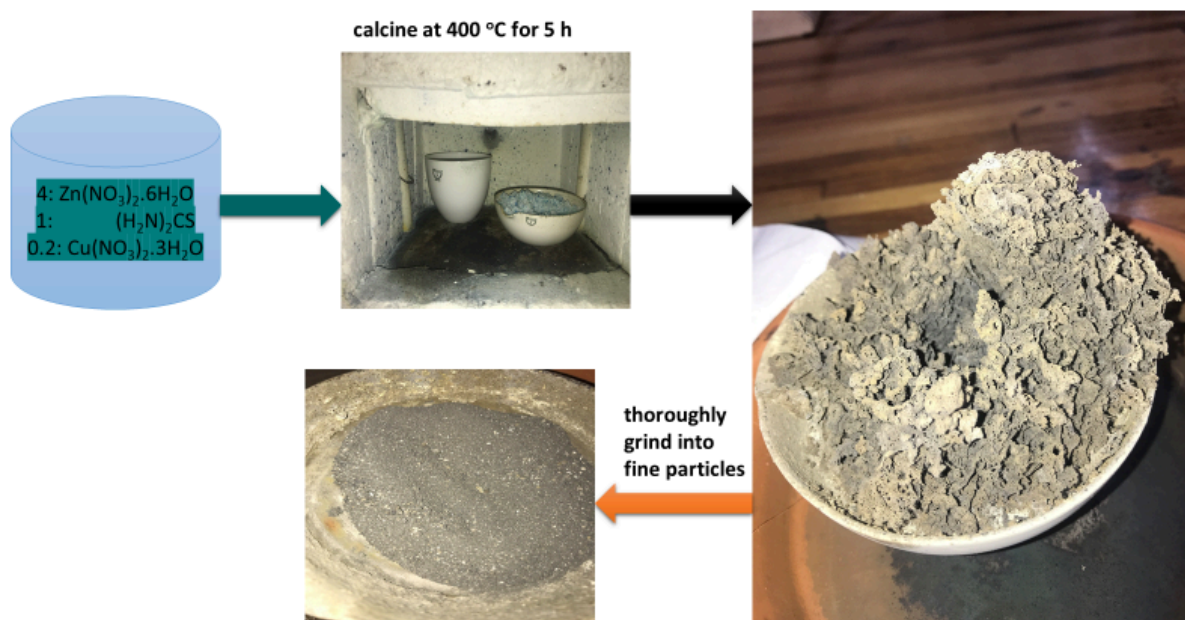


Figure 3.1: Solid phase one – pot CuS/ZnS catalyst synthesis.

Table 3.1: Absorbance values of the prepared standards.

| Concentration (ppm) | Run 1 | Run 2 | Run 3 | Run 4 | Run 5 | Average absorbance (a.u.) |
|---------------------|-------|-------|-------|-------|-------|---------------------------|
| 100 | 0.993 | 0.99 | 0.988 | 0.987 | 0.988 | 0.9892 |
| 70 | 0.744 | 0.743 | 0.741 | 0.74 | 0.741 | 0.7418 |
| 50 | 0.61 | 0.607 | 0.606 | 0.604 | 0.608 | 0.607 |
| 30 | 0.343 | 0.343 | 0.34 | 0.339 | 0.339 | 0.3408 |
| 10 | 0.132 | 0.13 | 0.131 | 0.129 | 0.127 | 0.1298 |
| 5 | 0.098 | 0.098 | 0.099 | 0.095 | 0.095 | 0.097 |

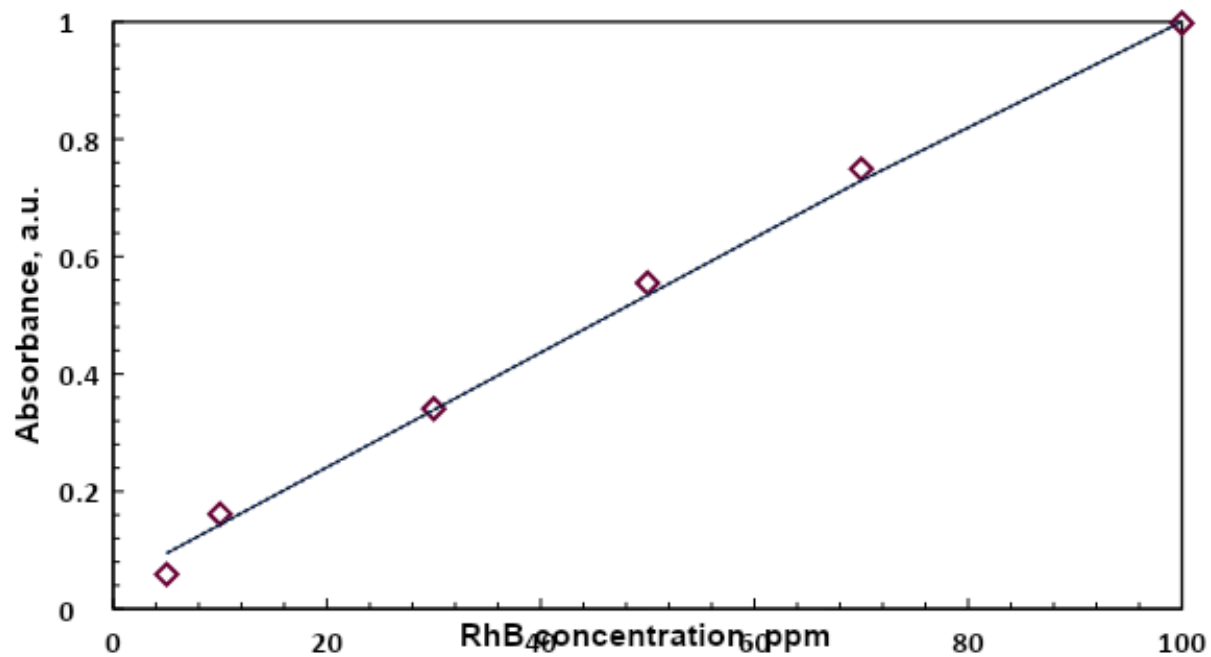


Figure 3.2: Calibration curve for RhB dye detection.

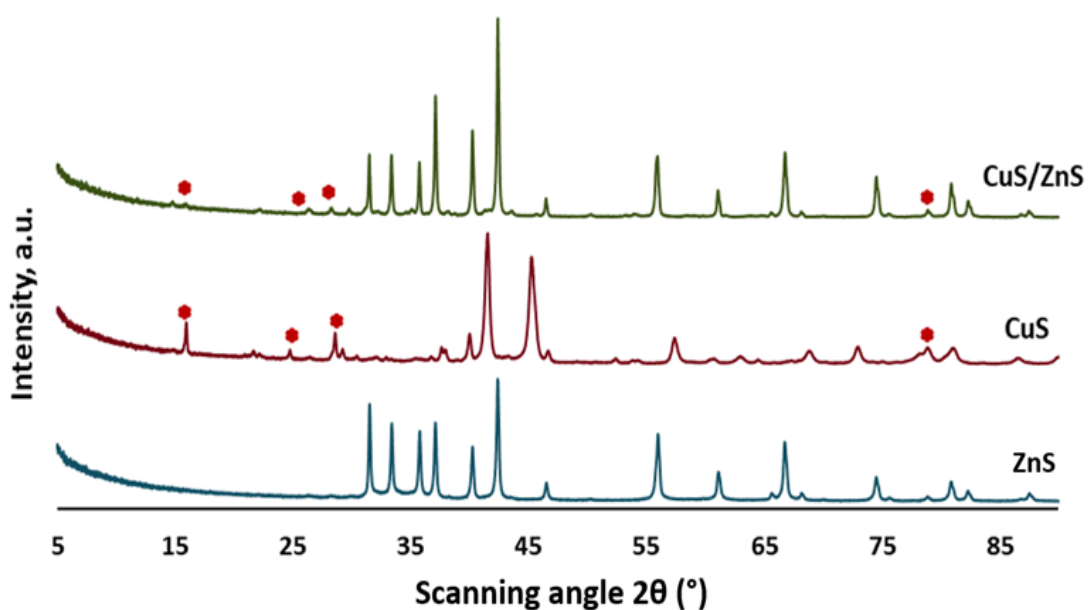


Figure 4.1: XRD patterns of the pristine ZnS and CuS as well as the CuS/ZnS composite.

Table 4.1: X-ray florescence data for synthesised materials.

| Component | ZnS | CuS | CuS/ZnS |
|--------------------------------|------------|------------|------------|
| Zn | 79.38 | 3.08 | 76.02 |
| Cu | 0.04 | 80.30 | 3.87 |
| S | 19.79 | 16.01 | 18.88 |
| Na ₂ O | 0.46 | 0.51 | 0.95 |
| MgO | 0.21 | - | 0.20 |
| Al ₂ O ₃ | 0.07 | 0.07 | 0.04 |
| CaO | 0.05 | 0.03 | 0.04 |
| TOTAL | 100 | 100 | 100 |

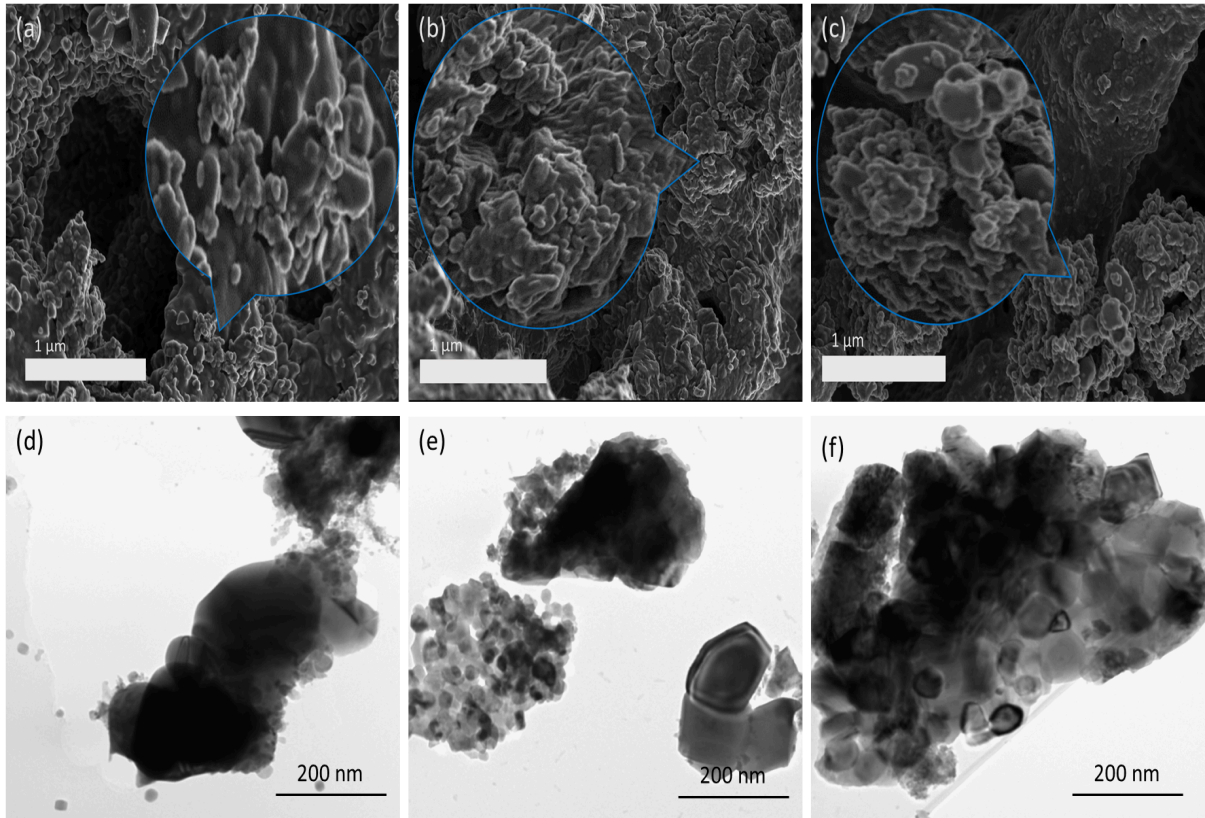


Figure 4.2: SEM images of (a) ZnS, (b) CuS, and (c) CuS/ZnS, and TEM images of (d) ZnS, (e) CuS, and (f) CuS/ZnS.

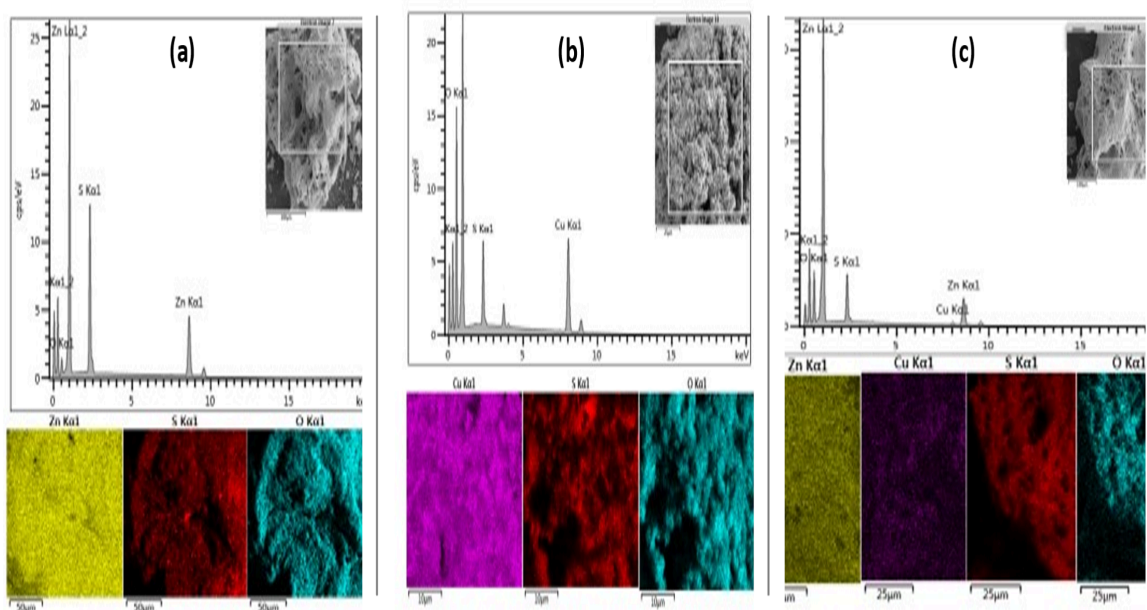


Figure 4.3: EDS elemental analysis and mapping of (a) ZnS, (b) CuS, and (c) CuS/ZnS.

Table 4.2: BET analysis surface area and pore size distribution of sorbents.

| Materials | Surface area (m ² g ⁻¹) | Average pore size (nm) | BJH Adsorption (4V/Å)* | BJH Desorption (4V/Å)* |
|-----------|---|---------------------------|------------------------------|------------------------------|
| ZnS | 4.06 | 12.03 | 73.47 | 75.61 |
| CuS | 8.73 | 11.22 | 60.68 | 82.43 |
| CuS/ZnS | 2.72 | 8.57 | 51.35 | 54.38 |

*Average pore width

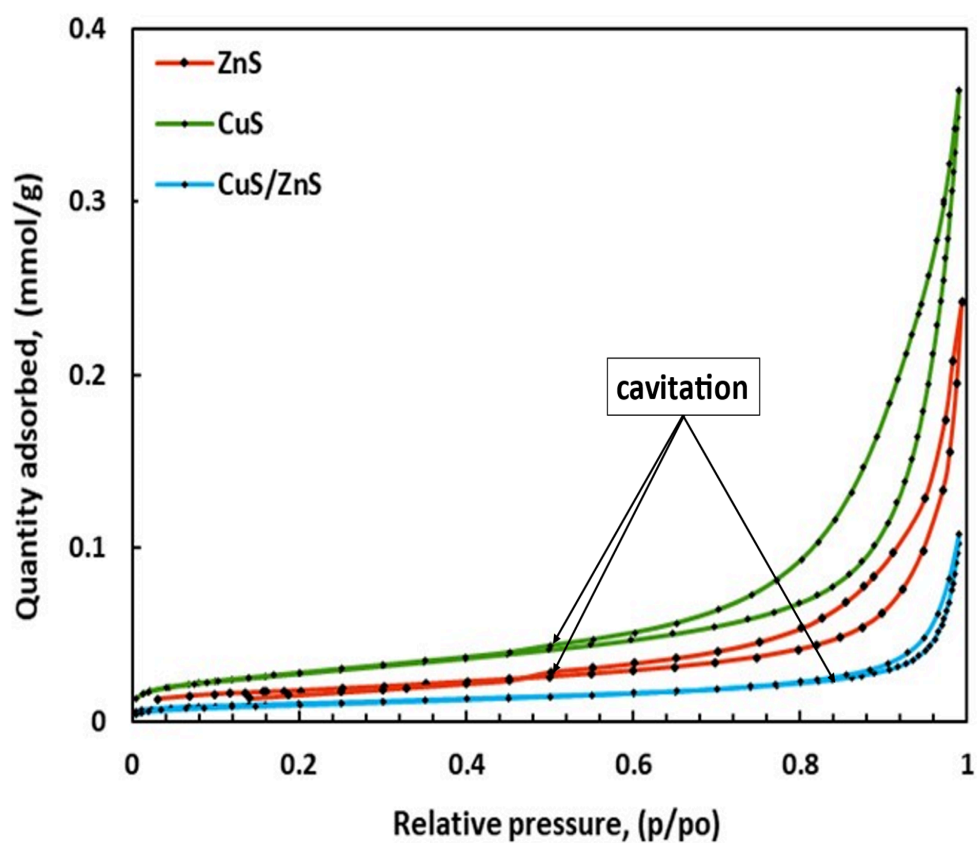


Figure 4.4: N₂ adsorption – desorption isotherm of synthesised catalysts.

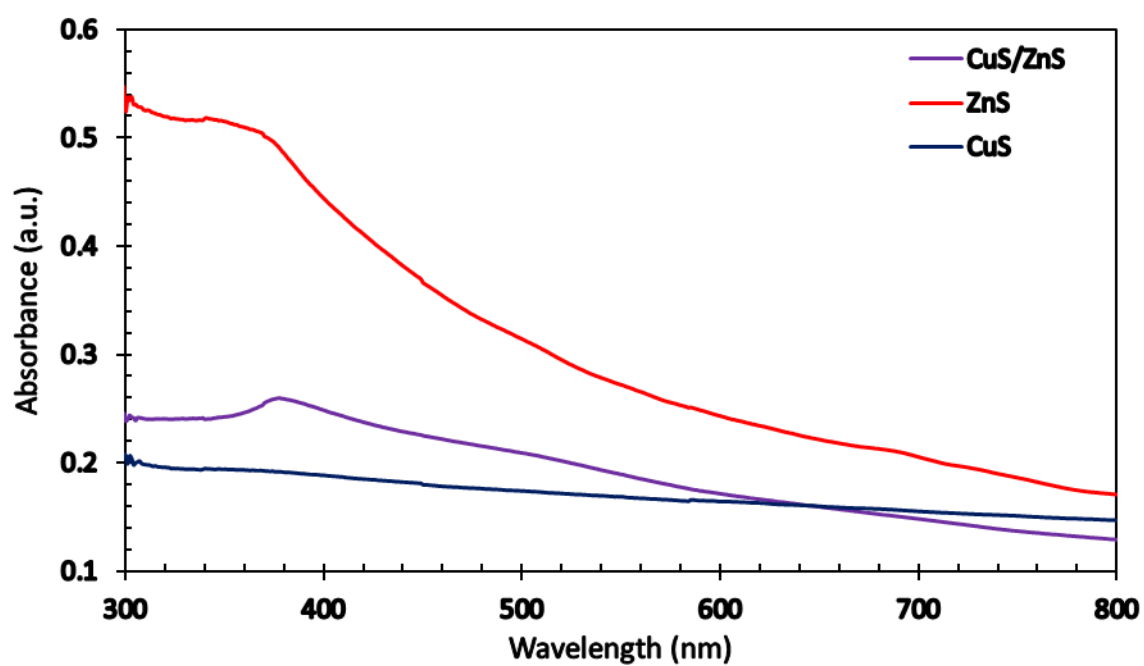


Figure 4.5: UV – vis absorption spectra of synthesised nanoparticles.

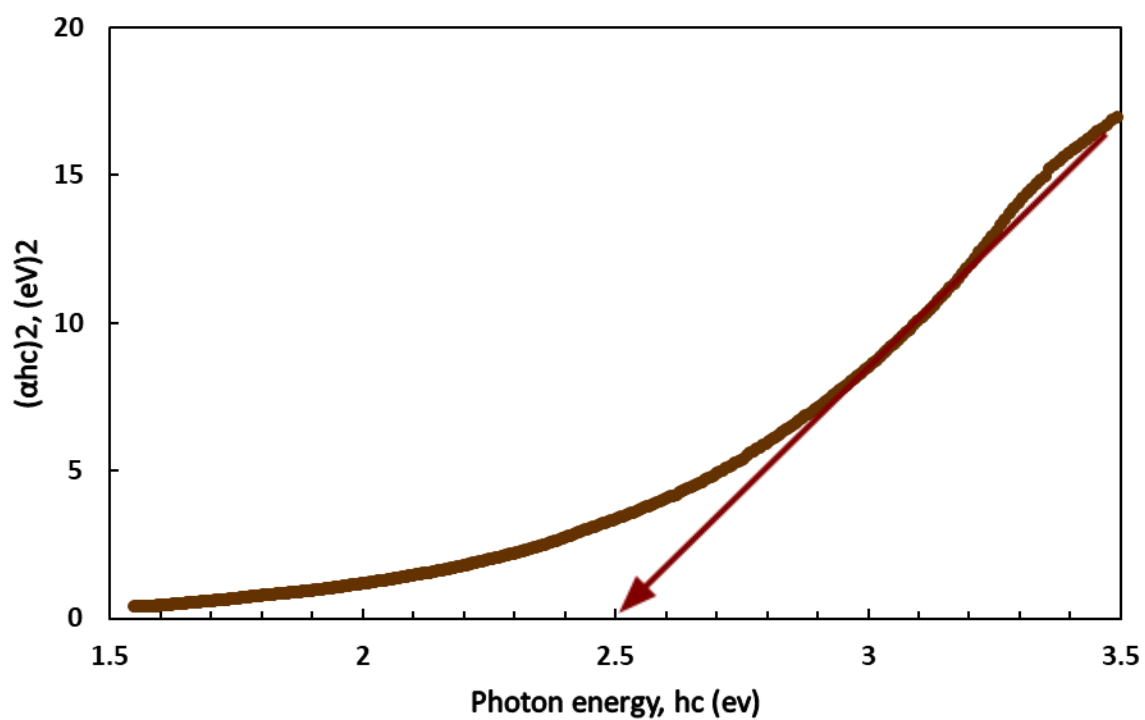


Figure 4.6: Tauc plot and estimated band gap for ZnS.

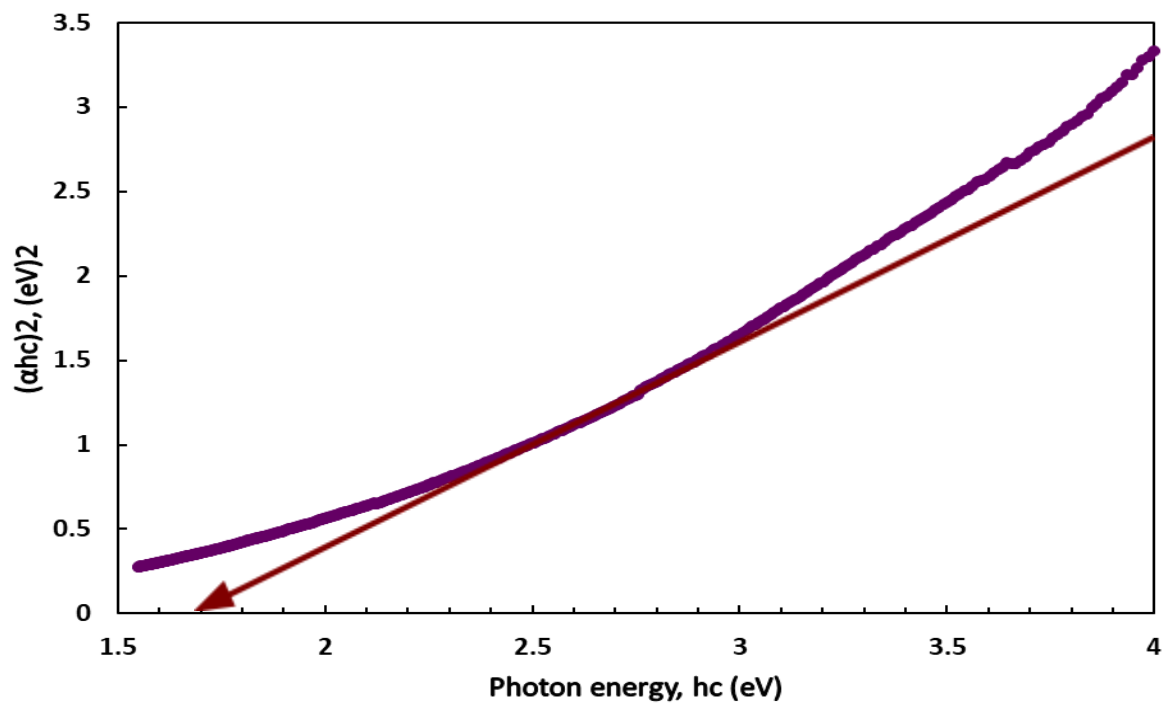


Figure 4.7: Tauc plot and estimated band gap for CuS.

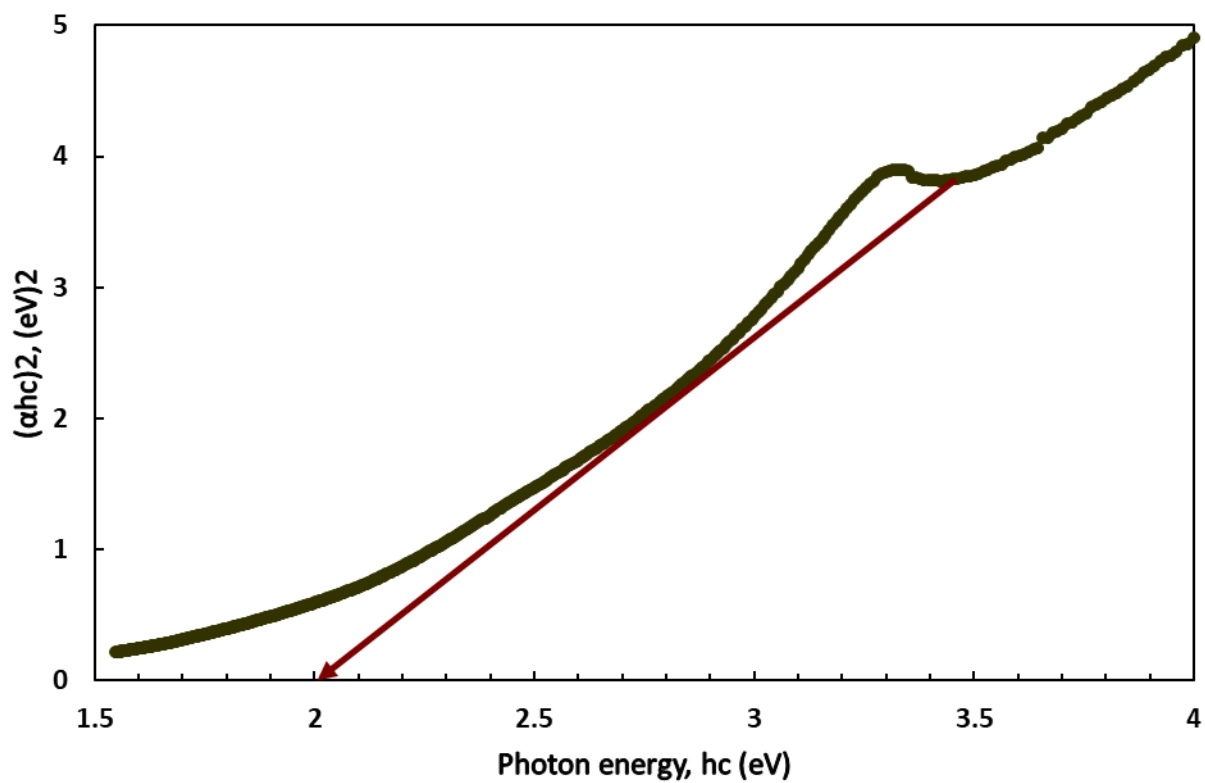


Figure 4.8: Tauc plot and estimated band gap for CuS/ZnS.

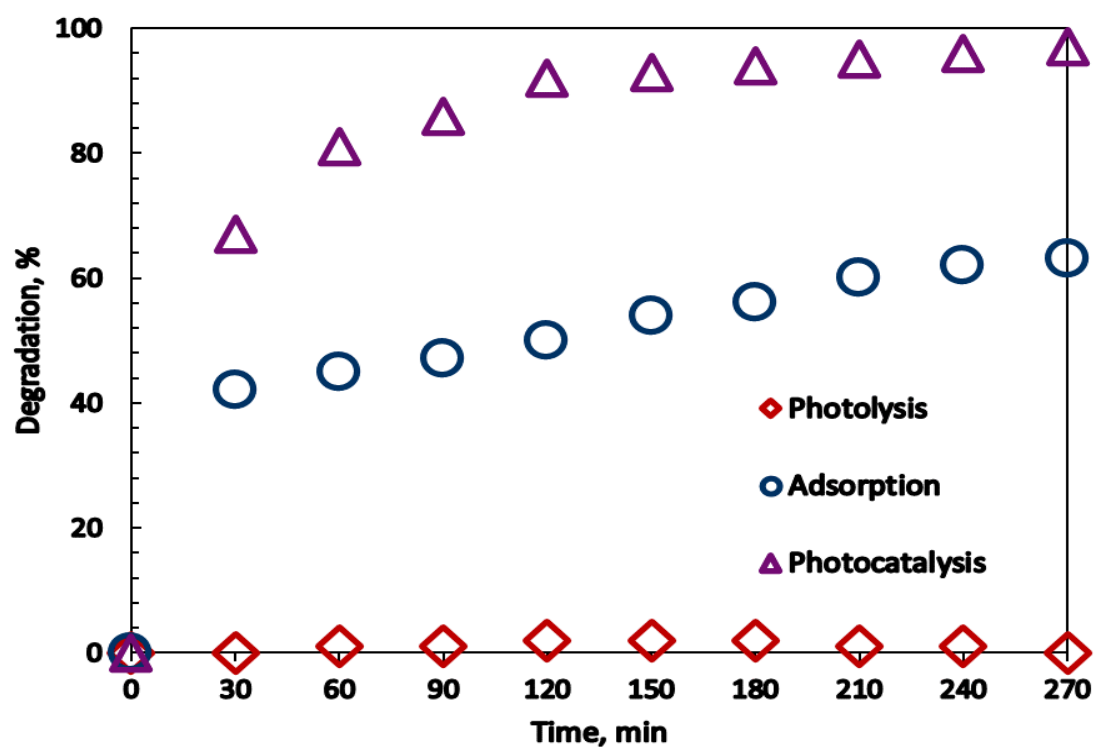


Figure 5.2: Control tests and photocatalysis of CuS/ZnS under visible light irradiation.

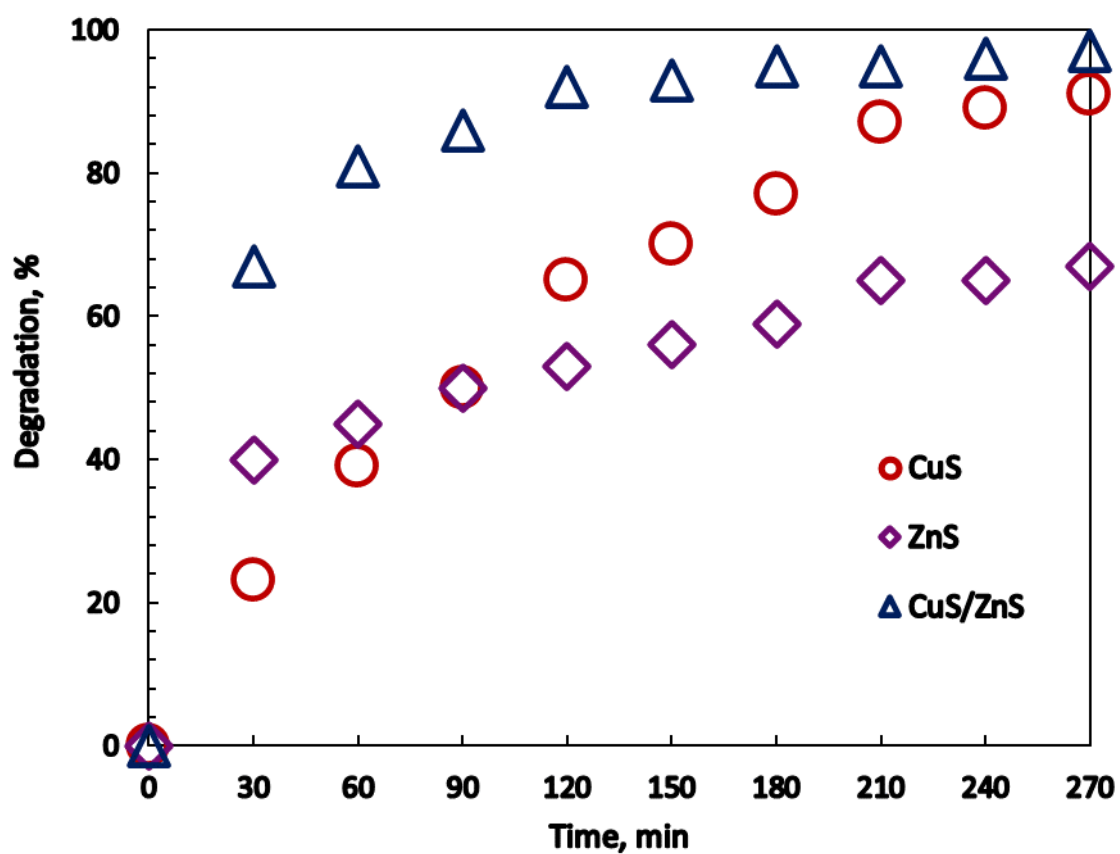


Figure 5.3: Performance of 10 gL^{-1} constituent catalyst on 5 ppm RhB dye solution.

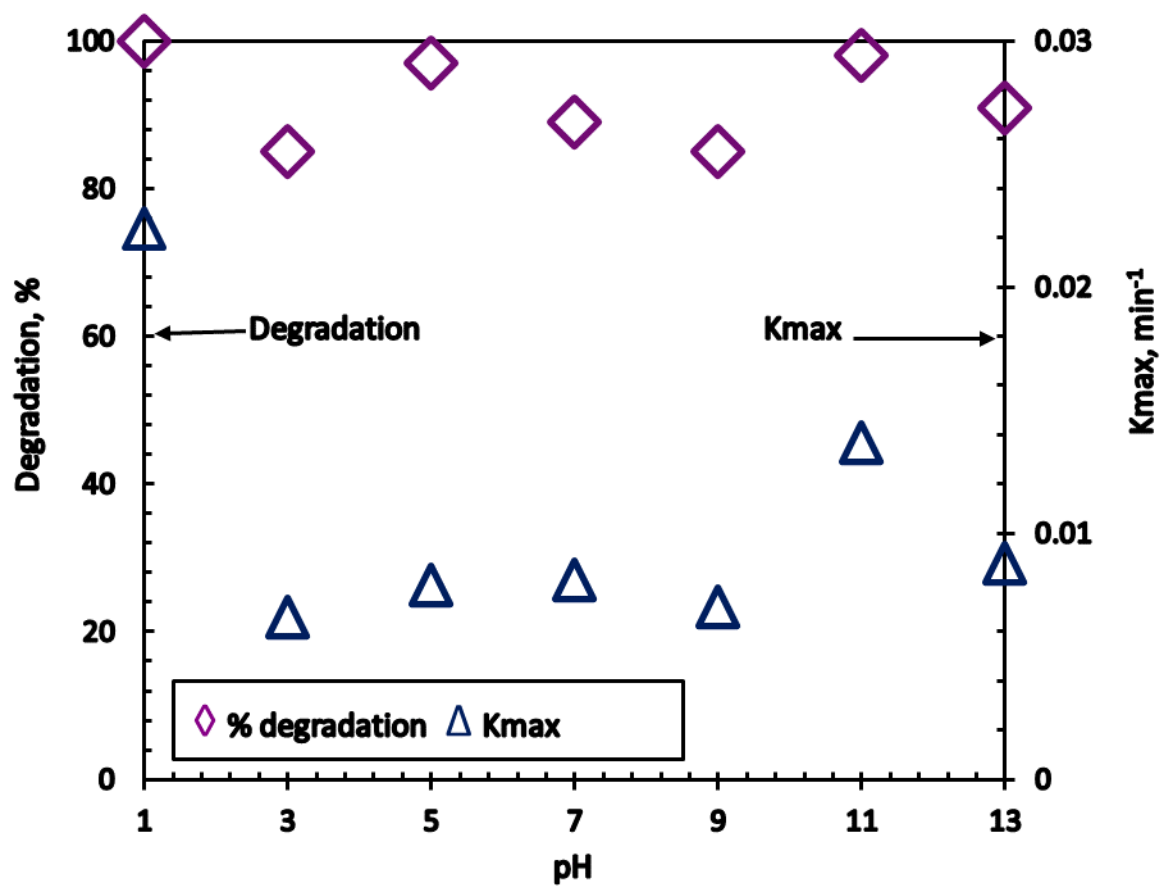


Figure 5.4: Reaction kinetics and effect of initial pH in RhB dye degradation with CuS/ZnS photocatalyst.

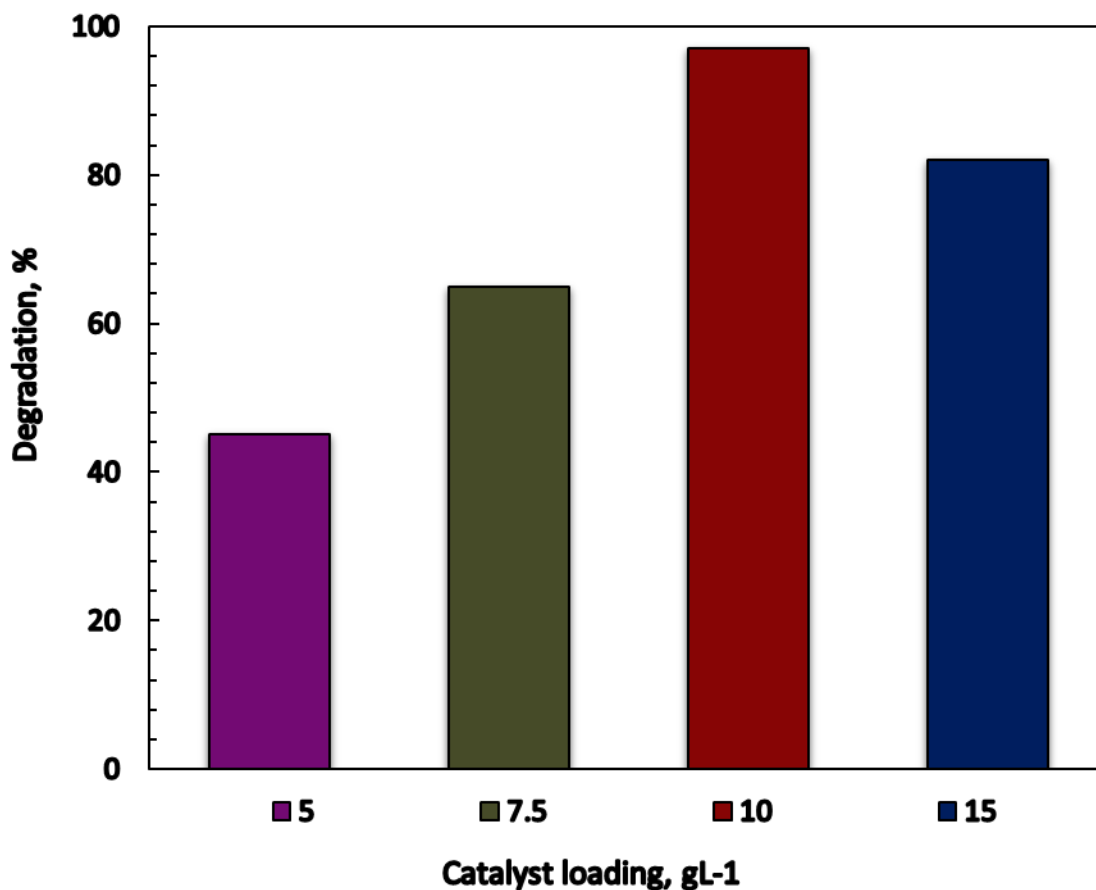


Figure 5.5: Effect of CuS/ZnS catalyst loading in RhB dye degradation.

Table 5.1: Photodegradation reaction kinetic parameters for varying binary CuS/ZnS nanocomposite catalyst loading in RhB dye degradation.

| Catalyst loading (gL ⁻¹) | Linear regression (R ²) | K _{max} (min ⁻¹) |
|--------------------------------------|-------------------------------------|---------------------------------------|
| 0 | 0.097 | 0.0000 |
| 5 | 0.897 | 0.0034 |
| 7.5 | 0.947 | 0.0058 |
| 10 | 0.986 | 0.0186 |
| 15 | 0.905 | 0.0094 |

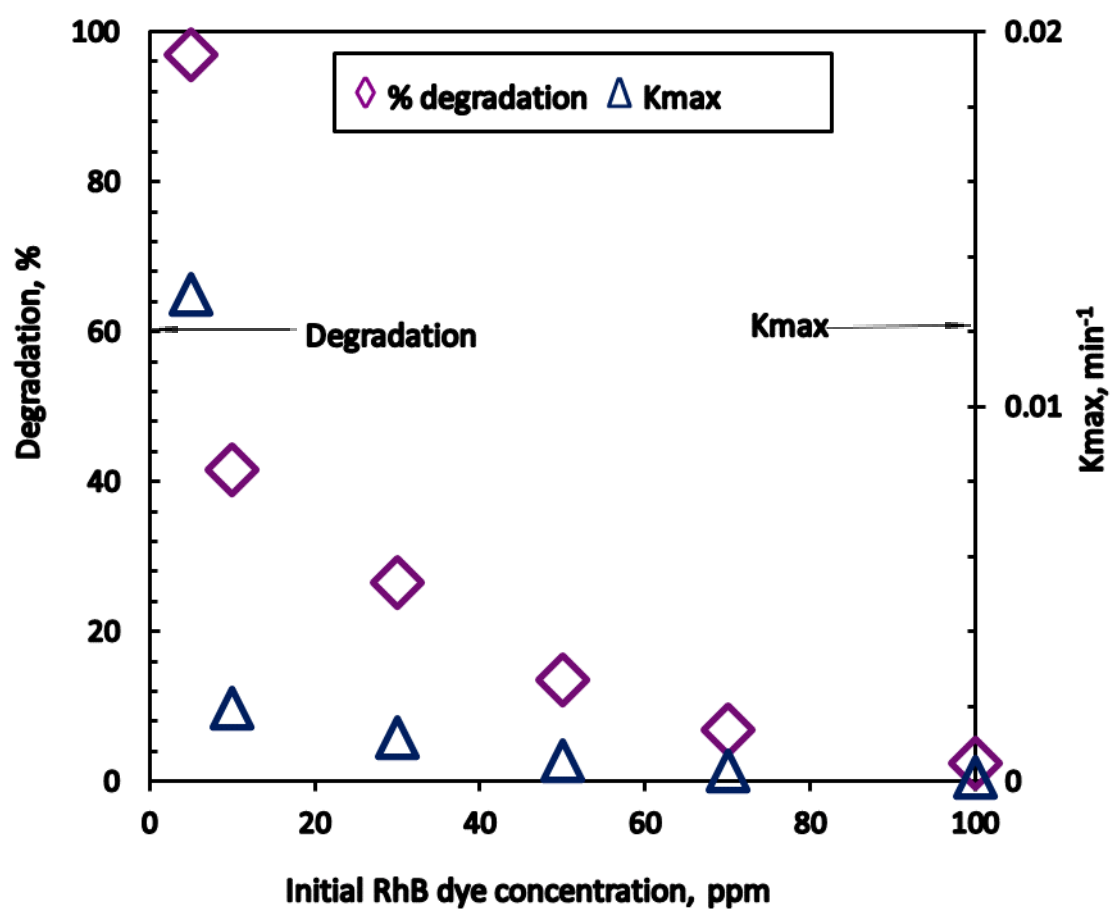


Figure 5.6: Reaction kinetics and effect of catalyst loading in rhodamine B dye degradation with CuS/ZnS photocatalyst.

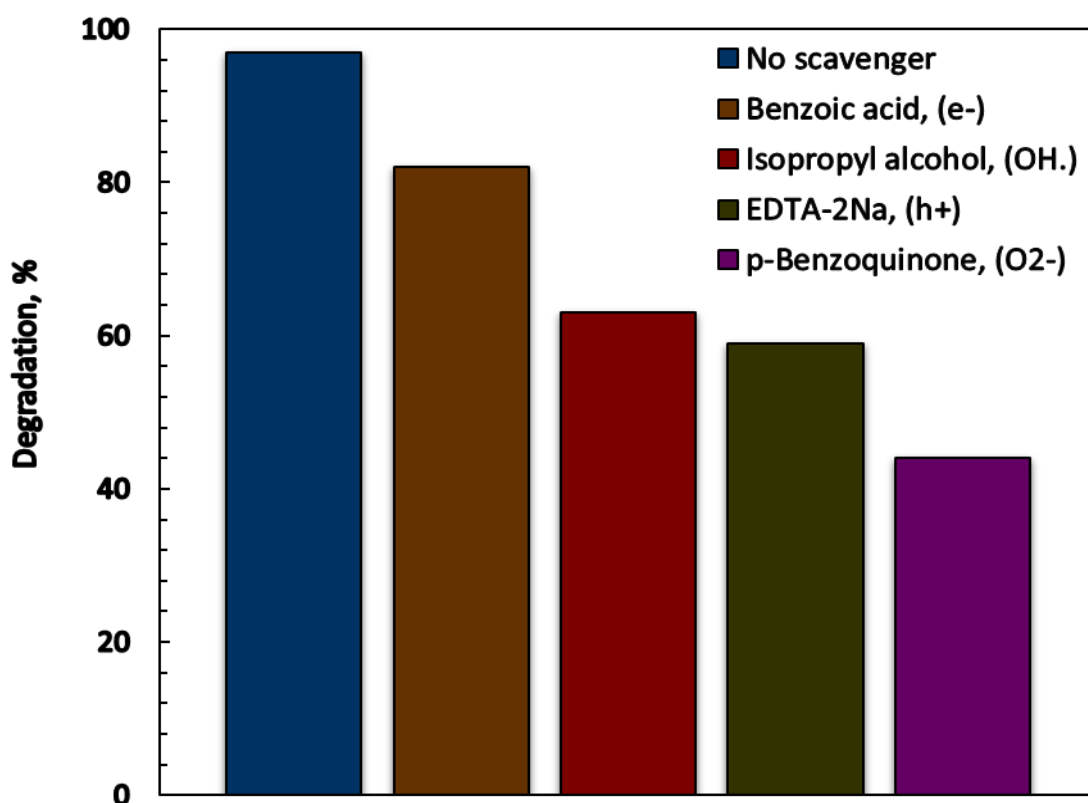


Figure 5.7: Effect of BA, IPA, EDTA – 2Na and pBZQ scavengers rhodamine B dye degradation efficacy using CuS/ZnS photocatalyst.

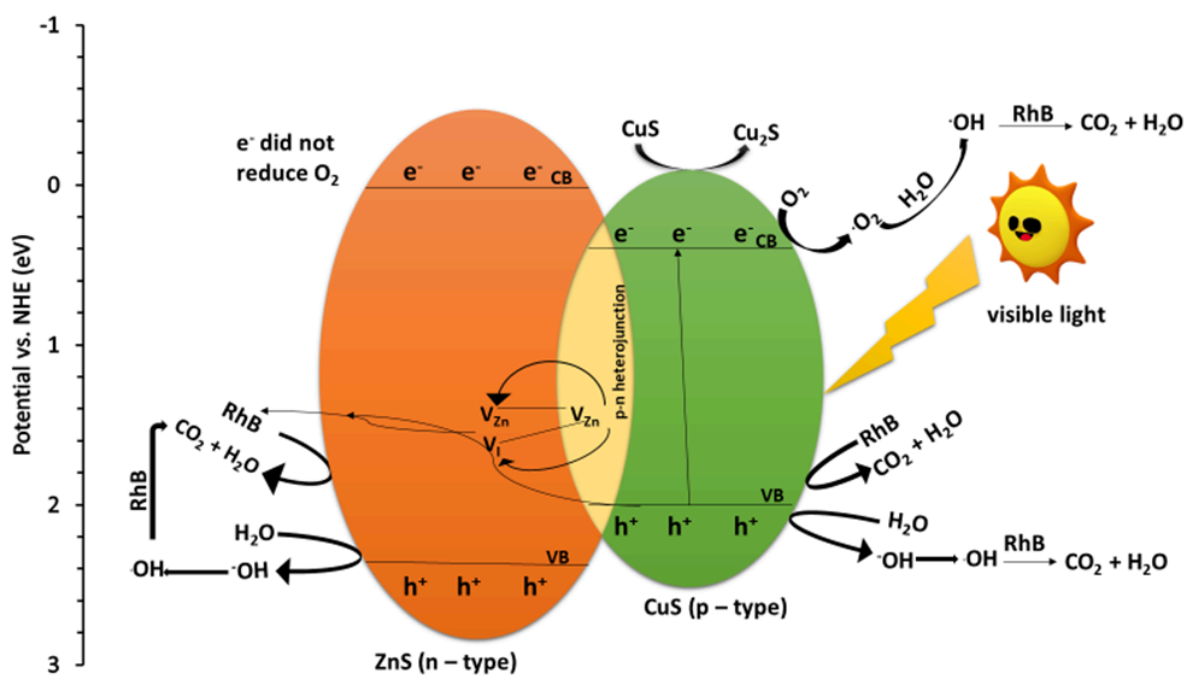


Figure 5.8: Proposed schematic representation of a p-n CuS/ZnS heterojunction photocatalytic mechanism.

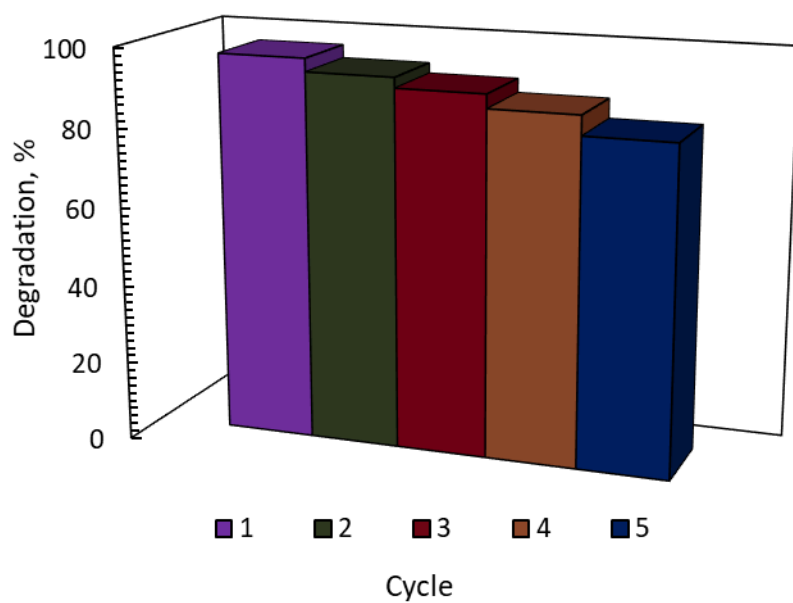


Figure 5.9: Stability and recyclability of CuS/ZnS photocatalyst during 5 cycles.

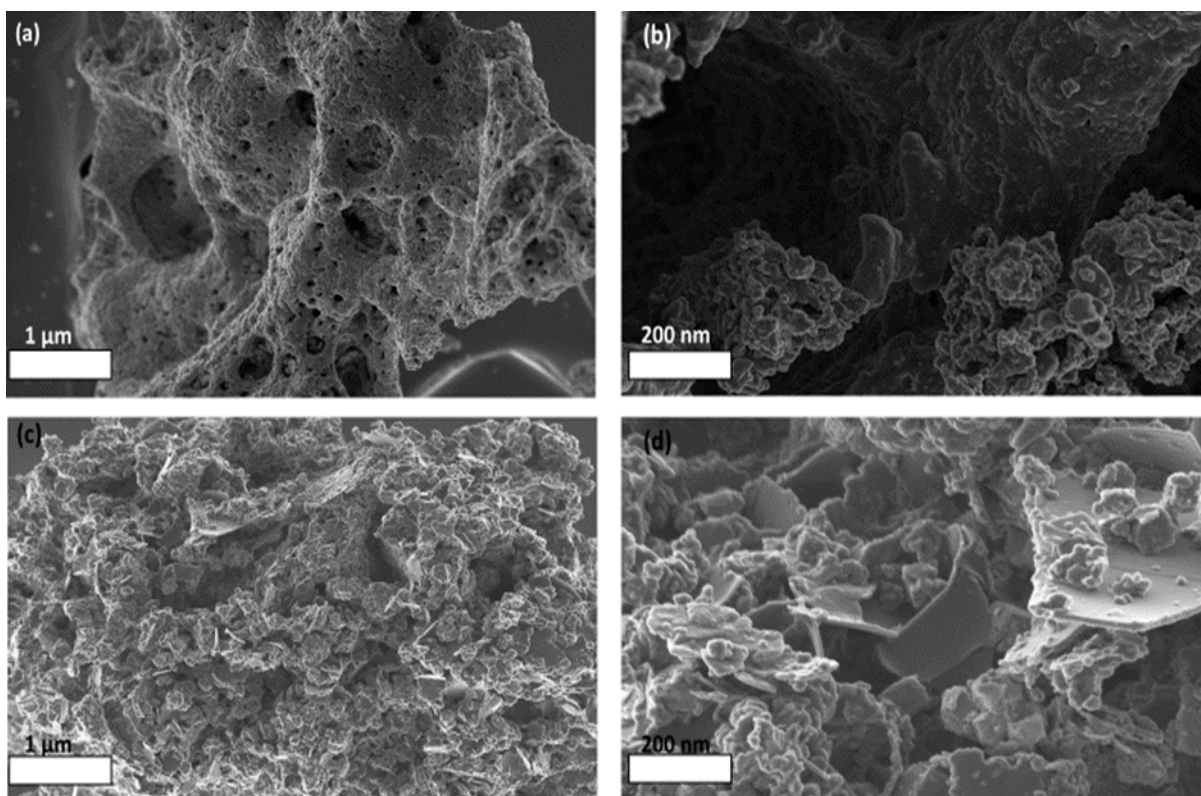


Figure 5.10: (a) Zoomed-out and (b) zoomed-in CuS/ZnS SEM images before use and (c) zoomed-out and (d) zoomed-in CuS/ZnS SEM images after 5 recycles.